




Investigation of the Variability of Near-Surface Temperature Anomaly and Its Causes Over the Tibetan Plateau

Ye Liu¹ , Yongkang Xue¹ , Qian Li², Dennis Lettenmaier¹ , and Ping Zhao³

¹Department of Geography, University of California Los Angeles, Los Angeles, CA, USA, ²Institute of Atmospheric Physics, Chinese Academy of Sciences, Beijing, China, ³State Key Laboratory of Severe Weather, Chinese Academy of Meteorological Sciences, Beijing, China

Key Points:

- Land surface temperature anomaly can sustain for seasons and is accompanied by persistent subsurface temperature, snow and albedo anomalies
- With middle-layer subsurface temperature as predictor, land surface temperature is highly predictable, especially during the springtime
- Soil properties and soil column depth predominate subsurface temperature memory, which suggests the key processes to improve its prediction

Supporting Information:

- Supporting Information S1

Correspondence to:

Y. Liu,
liuye.923@ucla.edu

Citation:

Liu, Y., Xue, Y., Li, Q., Lettenmaier, D., & Zhao, P. (2020). Investigation of the variability of near-surface temperature anomaly and its causes over the Tibetan Plateau. *Journal of Geophysical Research: Atmospheres*, 125, e2020JD032800. <https://doi.org/10.1029/2020JD032800>

Received 23 MAR 2020

Accepted 18 SEP 2020

Accepted article online 23 SEP 2020

Abstract Recent research has reported the great influence of springtime land surface temperature (LST) and subsurface temperature (SUBT) over the Tibetan Plateau (TP) on downstream region summer precipitation, indicating the potential application of LST/SUBT on subseasonal to seasonal (S2S) prediction. In this study, we employed both observational data and offline model simulation to explore the memory of surface and subsurface variables and assess the driving effects of snow/albedo and SUBT on the LST anomaly. Our composite analysis based on observation shows that the anomalous LST in the TP can sustain for seasons and is accompanied by persistent SUBT as well as snow and associated surface albedo anomalies. A multilayer frozen soil model reproduces the observed LST anomaly and shows surface albedo and middle-layer SUBT have 1–3 months memory, indicating the degree of persistence or dissipation of anomaly through time with more extended memory during spring. With simulated middle-layer SUBT as a predictor, the linear regression model produces R_{adj}^2 of 0.44 and 0.26 for 1- and 2-month LST prediction, respectively. The predictability is higher during the spring. Our results also show February snowfall, May snowmelt, and aero in snow exert substantial impacts on springtime LST through snow albedo feedback. The long memory of SUBT allows it to preserve the surface thermal anomaly and release it gradually in the following months to seasons. Meanwhile, the sensitivity study indicates that the soil properties and soil column depth predominate SUBT memory, which suggests the key processes to improve LST/SUBT then downstream S2S prediction.

1. Introduction

The Third Pole (Yao et al., 2019) exerts major control on the atmospheric circulation at local and continental scales. Tibetan Plateau (TP) surface processes play an important role in regional climate and in subseasonal to seasonal (S2S) prediction of extreme climate events such as droughts and floods (Lau & Kim, 2018; Li et al., 2018; Wang et al., 2008; Wu et al., 2016; Xiao & Duan, 2016; Xue et al., 2017, 2018). The relationship between snow in the TP and Indian and Asian monsoon variability has been identified for decades (Bamzai & Shukla, 1999; Dey & Bhanu Kumar, 1983; Fasullo, 2004; Kripalani et al., 2003; Wu & Qian, 2003). The TP snow cover anomaly, which is highly correlated with Eurasian snow cover (Bamzai & Shukla, 1999; Vernekar et al., 1995) and the Arctic Oscillation (Wang et al., 2019; Zhang et al., 2019), has shown influence on multiscale variations of South and East Asia (Wu & Kirtman, 2007; Yao et al., 2019). However, studies have shown that the snow-monsoon relationship in the TP is highly variable in time and space, especially as the spatial distribution of snow is gigantically heterogeneous during the spring melting (Bamzai & Shukla, 1999; Wu & Qian, 2003; Xiao & Duan, 2016), suggesting the difficulty of using TP snow cover directly as a predictor for drought/flood events. Moreover, in a study on the relationship between winter snow anomaly and spring and summer soil moisture (SM), Robock et al. (2003) reported that the prolonged snow albedo impact is not realized through SM feedback because the persistence of SM anomaly is too short to sustain its effect in the summer season. Xue et al. (2018) therefore conjectured that a temporally filtered response to the snow anomalies may be preserved in the land surface temperature (LST), which may contribute to the S2S prediction. The relationship between snow cover and LST anomalies had been a subject in a number of studies (Groisman et al., 2004; Park et al., 2014; Zhang, 2005; Zhang et al., 2019).

Xue et al.'s (2018) conjecture is based on the significant lagged correlation between spring air temperature (T_{air}) over the northern Rocky Mountain areas in North America and the TP in East Asia and their respective summer precipitation in their downstream regions. Although T_{air} anomaly in spring directly interacts with atmospheric circulation and precipitation, Xue et al. (2016, 2018) and Diallo et al. (2019) found that specifying proper initial LST and subsurface temperature (SUBT) is the only way to reproduce the observed persistence in the climate models. Their observational analyses and model sensitivity experiments show that the T_{air} /LST/SUBT effect is comparable to or in some areas/seasons probably more important than the well-known sea surface temperature effects. As such, it is important to understand the sources, characteristics, and memory of the LST/SUBT anomalies. Zhang et al. (2019) reported that spring LST in the TP is coupled with the regional snow cover in preceding months, while the latter is influenced by wave activities in middle to high latitudes. Due to the importance of S2S prediction, a multimodel project under the Global Energy and Water Exchanges project (GEWEX) and the Third Pole Environment (TPE) support has been initiated to further investigate the impact of initialized LST and snowpack on subseasonal to seasonal prediction (LS4P) (Xue, Boone, et al., 2019; Xue, Lau, et al., 2019). To investigate the LST anomaly in the TP and its impact on downstream precipitation, it is necessary to understand the characteristics of the LST anomaly and its causes. Thus far, a common shortcoming in the LS4P models has been their deficiency in maintaining the LST anomaly as long as observations. This problem may be rooted in the deficiency in producing proper soil temperature memory and land/atmosphere interaction. The “soil temperature memory” refers to the degree of persistence (high memory) or dissipation (low memory) of a soil temperature anomaly through time (Hu & Feng, 2004a). Hu and Feng (2004b) analyzed the variation of soil enthalpy, which represents the integration of soil temperature through the soil column. Using soil temperature observations from 292 stations in the United States, they found that the soil enthalpy anomaly in the top 1-m soil column could persist for 2–3 months. The seasonal-scale thermal inertia indicates that soil thermal processes could “record” atmospheric circulation anomalies and “release” their effects in the following months, highlighting the S2S predictability and the importance of SUBT initialization. Improving the SUBT memory simulation provides a feasible approach to extending LST anomaly persistence in LS4P models.

The SUBT directly affects the LST through heat transport and surface energy budget. Wu and Zhang (2014) used a regional climate model to show that the SUBT plays an important role in amplifying summer LST variability over the arid and semiarid regions of East Asia. Mahanama et al. (2008) reported that interactive SUBT significantly increases LST variability and persistence in most regions, by using an atmospheric general circulation model. In addition, Yang and Zhang (2016) further showed that the SUBT memory is seasonally dependent. However, a comprehensive investigation of the various causes of LST anomaly has not been conducted; characteristics of SUBT memory and their association with snow persistence is not yet well understood.

The objective of this study is to explore various possible causes of the LST anomaly and its S2S predictability, with a particular focus on the impacts of SUBT memory and associating snow and surface albedo persistence. The remaining sections are arranged as follows: station observation, model simulation, and methods are introduced in section 2; section 3 describes the characteristics of the LST anomaly and its relationship to SUBT and snow anomalies, S2S predictability of LST, and the possible mechanism that SUBT and snow persistence affects LST variation; and conclusions and discussion are presented in section 4.

2. Data, Model Description, and Model Simulation

2.1. Station Observations

The observed LST data used in this study are the monthly mean surface temperature recordings of 80 stations over the TP covering the period of 1961–2017, provided by the China Meteorological Administration (CMA, <https://data.cma.cn>). The geographical locations of the station are shown in supporting information Figure S1. Those stations also recorded snow depth from 1973 to 2014 (Zhao et al., 2007). Fourteen stations (indicated by squares in Figure S1) have soil temperature measurements during 1981–2005 at depths of 0, 5, 10, 15, 20, 40, 80, 160, and 320 cm. The station observations during the overlapping period, that is, 1981–2005, are analyzed in this study.

2.2. Gridded Data

CMA provides monthly gridded LST observations over China for the period of 1961–2017. The observations were interpolated from about 2,400 stations by using Thin Plate Spline algorithm to 0.5° spatial resolution (data are available at <https://data.cma.cn>).

The surface albedo product from Global Land Surface Satellite (GLASS), covering 1981–2017, was generated from the Advanced Very High Resolution Radiometer (AVHRR) observations (1981–2000) and data from the Moderate Resolution Imaging Spectroradiometer (MODIS) sensors onboard the Terra and Aqua satellites for the period of 2000 to 2010 (Liu et al., 2013) (available at <http://www.glass.umd.edu>). The original GLASS albedo data are at 0.05° spacing resolution, which is resampled to 0.5° resolution by using a bilinear interpolation algorithm.

The meteorological forcing data provided by the Chinese Academy of Sciences were used to drive the offline model in this study (Yang et al., 2010). This data set contains variables of downward shortwave radiation (W m^{-2}), downward longwave radiation (W m^{-2}), precipitation (mm day^{-1}), air temperature (K), relative humidity (kg kg^{-1}), air pressure (Pa), and wind speed (m s^{-1}). The data set is based on existing data, such as Princeton reanalyzed data, the Global Land Data Assimilation System (GLDAS) materials, GEWEX Surface Radiation Budget (SRB) radiation data, and the Tropical Rainfall Measuring Mission (TRMM) precipitation data, which are integrated with regular meteorological observations from CMA. The original spatial and temporal resolutions of this data set are 0.1° and 3-hourly, respectively, and were resampled to 0.5° spatial resolution via bilinear interpolation algorithm and to 1-hourly temporal interval via cubic spline interpolation algorithm.

2.3. Land Surface Model Description

The simplified simple biosphere model (SSiB) is a biophysically based land surface model that simulates fluxes of radiation, momentum, sensible heat, and latent heat fluxes, as well as runoff, SM, and surface temperature (Xue et al., 1991). A multilayer frozen soil model (Li et al., 2010; Zhang et al., 2007) has been included in the SSiB version 3 (SSiB3) and referred to as SSiB3-FSM. This model consists of 8–12 layers with the total soil column depth from 2.5 to 11.7 m depending on land cover conditions. A semi-implicit scheme with more efficient computation and stable solutions has been introduced to solve the temperature, liquid water, and ice prognostic equations instead of enthalpy and total water mass in the frozen soil model, in which soil temperatures in multisoil layers are solved by a tridiagonal matrix. To better describe the soil temperature vertical profile, in this study we increase the number of soil layers to 120 for all land cover types with 0.05-m depth for each layer.

To investigate the effects of soil properties and upper and lower boundary conditions on soil thermal persistence, a simplified version of SSiB3-FSM, which eliminates all hydrologic processes, such as surface evaporation and snow accumulation and melting, is introduced and is referred to as SSiB3-Dry. SM and precipitation are also set to 0 when SSiB3-Dry is running.

Three sets of experiments were conducted in this study. In Exp-1, a spin-up run using SSiB3-FSM was first conducted, forced by 1979–1988 meteorological forcing repeatedly for 60 years to reach an equilibrium status. After that, a transient run for 1979–2015 was conducted, driven by historical forcing data from 1979–2015. In Exp-2 and Exp-3, short-term sensitivity simulations, the climatological forcing (averaged over 1979–2015) was used to drive SSiB3-FSM or SSiB3-Dry for 60 years to reach an equilibrium status. Two subsets are included in Exp-2 to investigate impact of anomalous snow, by replacing snow water equivalent (SWE) by the average of extreme warm/cold years, in each month from December through May, respectively. Exp-3 includes four subsets to evaluate the role of soil thermal diffusivity (Exp-3.2), snow cover (Exp-3.3), and total soil column depths (Exp-3.4) in preserving soil temperature anomaly, by comparing to the default model configuration (Exp-3.1). For each experiment in Exp-3, paired runs with/without a vertical homogenous 5°C anomaly initialization are conducted. The detailed settings of experiments are listed in Table 1.

2.4. Autocorrelation, Memory, and Lagged Cross Correlation

The autocorrelation of the anomalous time series, which is the departure from the long-term average, is used for this study. The autocorrelation coefficient is a direct measure of persistence. Quantitatively, the time scale

Table 1
Summary of Experiments

Experiment	Model	Spin-up	Description
Exp-1	SSiB3-FSM	1979–1988 cycling forcing for 60 years	Long-term experiment from 1979–2015
Exp-2			
SWE-warm	SSiB3-FSM	1979–2015 climatology for 60 years	Driven by climatological forcing. Integration from December to May, with SWE replaced by the average of extreme warm years, in December through May, respectively.
SWE-cold	SSiB3-FSM	The same as SWE-cold	The same as SWE-warm, except that SWE is replaced by the average of extreme cold years in December through May.
Exp-3			
Exp-3.1	SSiB3-Dry	1979–2015 climatology for 60 years	Driven by climatological forcing for 1 year. Two runs (control/sensitivity) without/with a vertical homogenous 5°C anomaly imposed
Exp-3.2	SSiB3-Dry	The same as Exp-3.1	The same as Exp-3.1, except reduced soil diffusivity in the sensitivity run
Exp-3.3	SSiB3-Dry	The same as Exp-3.1	The same as Exp-3.1, except 2-m snow cover imposed in the sensitivity run
Exp-3.4	SSiB3-Dry	The same as Exp-3.1	The same as Exp-3.1, except reduced soil column depths in the sensitivity run

that anomaly can persist, also known as memory, is defined as the time required for the lagged autocorrelation to drop below the 99% confidence level (Dirmeyer et al., 2009). We compute the monthly lagged autocorrelation curves of both observed and simulated anomalies to assess their persistence qualitatively and compute the daily lagged autocorrelation of simulated anomalies to determine their memory quantitatively. The lagged cross correlation is also calculated to explore the possible causal relationship from one variable to the other. The two-tailed t test is used to determine the significance of the correlation coefficient in this study.

2.5. Linear Regression Model

To assess the LST (T_s) prediction skill using SUBT and snow anomalies as predictors, a linear regression model (LRM) is used to estimate T_s anomaly in the current month with predictors in the preceding month on each grid point over the TP. The LRM is written as

$$\hat{T}_s = \sum_{i=1}^n \hat{\beta}_i var_i + \hat{\beta}_0, \quad (1)$$

where var_i is the anomaly of the i th input variable in the previous month, for example, downward short-wave radiation (SW_{in}), downward longwave radiation (LW_{in}), surface albedo, and SUBT (T_g) in the previous month; $\hat{\beta}_i$ is the regression coefficient; and \hat{T}_s is the estimation of T_s . The adjusted R^2 (R_{adj}^2) is used to evaluate the model fit (the variance in the T_s accounted for by the predictors).

$$R_{adj}^2 = 1 - \frac{SSE/(n-p-1)}{SST/(n-1)}, \quad (2)$$

where SSE is the sum of squares of residuals, indicating the variance cannot be explained by LRM; SST is the total variance of T_s , $n-1$ is the degrees of freedom of T_s , and p is the number of input predictors. Meanwhile, an overall F test is applied to test the significance of the regression. We split the data into training set (70% of the record) and cross-validation set (30% of the record). The training set is used to determine $\hat{\beta}_i$ and R_{adj}^2 . The out-of-sample mean absolute error (MAE) and root-mean-square error (RMSE) are calculated using the cross-validation set to evaluate the predictability of the LRM.

3. Results

3.1. Climatology and Anomaly Characteristics of LST, SUBT, and Snow Depth

Annual mean LST over the TP decreases from east to west. Over the western TP, with elevations generally over 5,000 m, the annual mean LST is about -10°C , while it ranges from 0°C to 10°C in the eastern TP (Kuang & Jiao, 2016). In response to the solar radiation, the range of seasonal variation in the LST is about 40°C based on the station observations. The seasonal variation of SUBT averaged across all stations decreases with soil column depth (Figure 1). The temperature gradient results in downward soil heat

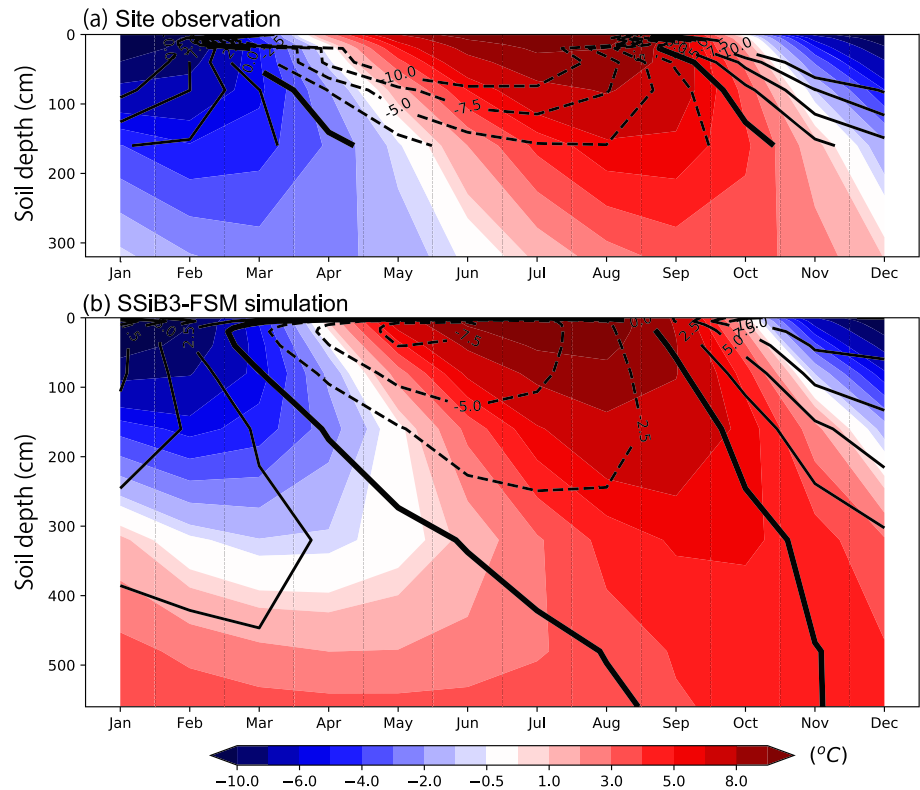


Figure 1. Climatology of soil temperature (shaded) and soil heat transport (contour) from (a) site observation and (b) SSiB3-FSM simulation. Dash contour indicates downward heat transport, while solid contour indicates upward heat transport.

transport in summer and upward transport in winter. There is a phase lag in SUBT annual cycle from the upper to deeper soil layer, and the lag period increases with soil column depth. In spring (March–April–May), the surface becomes warmer in response to increased downward radiation and reduced surface albedo, while the deeper soil is still cold. It leads to an enhanced soil heat flux gradient. The analogous condition occurs in fall but with opposite temperature gradient and energy transport direction.

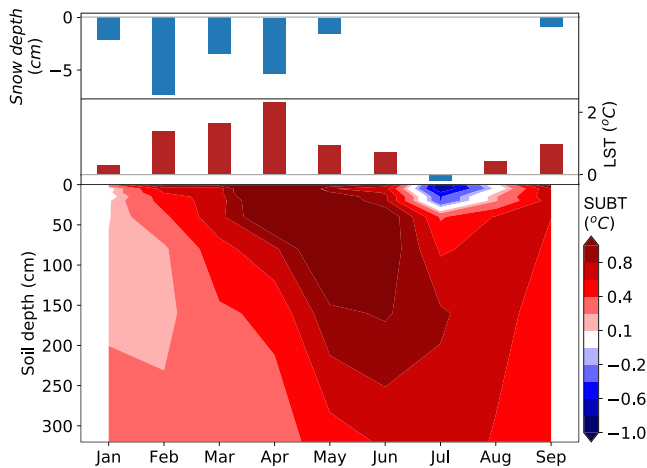


Figure 2. Observed difference in snow depth, LST, and SUBT between the years with warm and cold springs. The extreme warm/cold years are selected when the anomaly of the station-averaged LST is greater/less than half standard deviation.

To better illustrate the thermal characteristics of the TP, extreme warm/cold years, defined as spring LST anomaly averaged across the stations is greater/less than half of its standard deviation, are selected. Figure 2 shows the observed differences in LST, SUBT, and snow depth between the years with warm and cold springs. Although the extreme years are selected only based on spring LST, the warm LST signal starts in January, and it becomes warmer through February, March, and April. The anomalous warming lasts until September. The persistent warming LST is associated with less snow during winter and spring and persisting warm SUBT from January through September. Because of the interaction with atmosphere, anomalies in LST decay quite fast compared to that in SUBT. The warm core in the middle soil layer (40–160 cm) is about 1–2 months behind the surface and lasts for a longer period. Consequently, middle-layer SUBT becomes warmer compared to upper layer SUBT (20 cm) and LST from May to September, when the surface warm anomaly attenuates.

SSiB3-FSM simulation (Exp-1) averaged from the nearest grid points to the stations is capable of reproducing the climatological SUBT profile (Figure 1) and the persistent anomalies in LST, SUBT, and snow

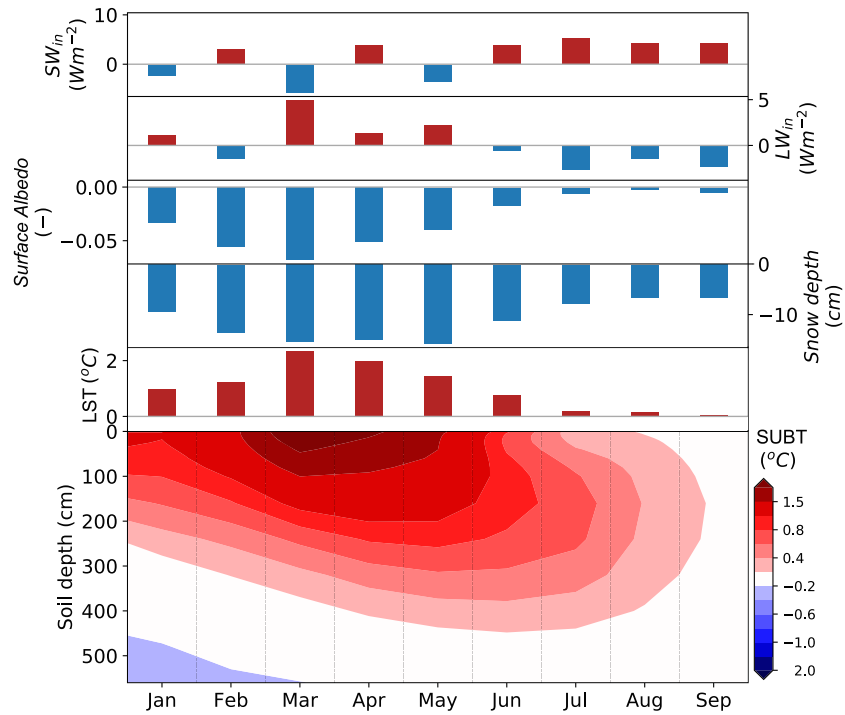


Figure 3. Simulated difference in SW_{in} , LW_{in} , surface albedo, snow depth, LST, and SUBT between the years with warm and cold spring. The extreme warm/cold years are selected when the anomalies over the TP are greater/less than half standard deviation.

(Figure S2). Over the whole TP, the composite analysis using Exp-1 outputs also shows that there are sustained LST, SUBT, and snow anomalies for the extreme years selected based on the LST anomaly in springs (Figure 3). Because of the closed snow and surface albedo relationship, that is, heavy snow normally is associated with high albedo, surface albedo also presents sustained negative anomaly associated with the warm LST. For downward shortwave and longwave radiations, which are two important energy sources for the surface, however, there are no persistent anomalies (Figure 3).

3.2. Relationships and Memory of LST, Surface Albedo, and SUBT

Anomalous LSTs are closely associated with persistent anomalies in SUBT, snow, and surface albedo (Figure 3). This section discusses their relationship and memory of surface albedo and SUBT through their lag correlation. Because the snow is absent during the summer in many years, we only focus on the anomaly in surface albedo in the following discussion. Based on the station observation averaged across all sites, the anomalous LST is significantly correlated to SUBT anomaly at all depths as well as surface albedo anomaly at 0- and 1-month lead (Figure 4a). At 0-month lead, the upper soil layer is the most interactive with the surface, with a correlation of 0.84 ($p < 0.01$). The correlations of LST to SUBT decrease with soil column depth. At 1-month lead, the correlation of LST to 20-cm SUBT reduces to 0.35 ($p < 0.01$). The correlations of LST to SUBT at the middle to subsurface layer (320 cm), however, are not significantly decayed at 1-month lead compared to correlations at 0-month lead. Consequently, at 1-month lead, the anomalous SUBT at the middle soil layers has the highest correlation to the LST anomaly (~ -0.44 , $p < 0.01$).

The lagged autocorrelation in each soil layer indicates the time period that the anomalies can be preserved in that layer. In general, the decay of SUBT autocorrelation curve at each layer is nearly monotonic according to the station observations (Figure 4b). The autocorrelation of the upper layer SUBT decays faster than that of middle to deeper layers. In general, the autocorrelation is not different from 0 ($p < 0.01$) after 3 months for the upper soil layers, while the autocorrelations in middle and deeper layers persist for a much extended period because the high-frequency fluctuation damps rapidly in soil and can only reach the shallow soil layers (Dickinson, 1988). The deeper soil column depth is, the slower anomaly attenuation rate and the larger

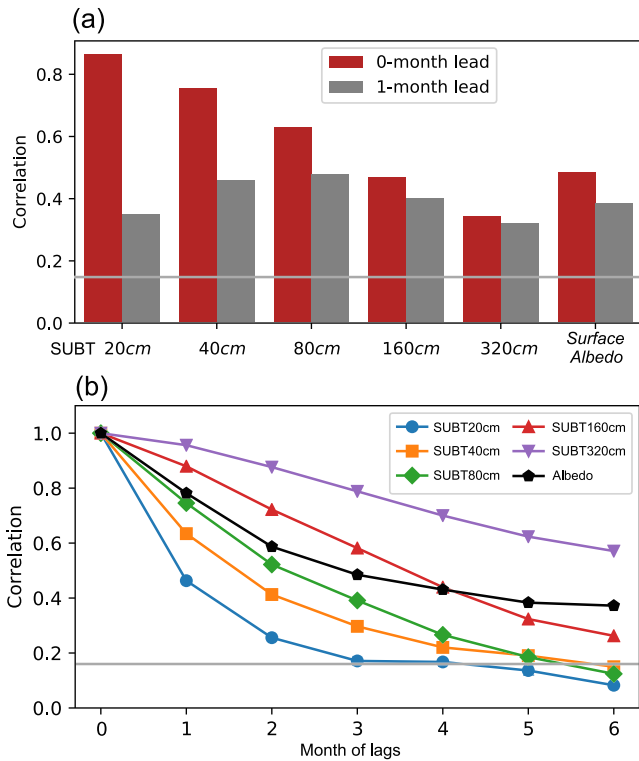


Figure 4. (a) Lagged cross correlation of LST to SUBT and surface albedo at 0- and 1-month lead. The time series is averaged across the stations with SUBT measurement. (b) Lagged autocorrelation of monthly anomalies in SUBT at different layers and surface albedo. The gray line indicates significance level of 0.01.

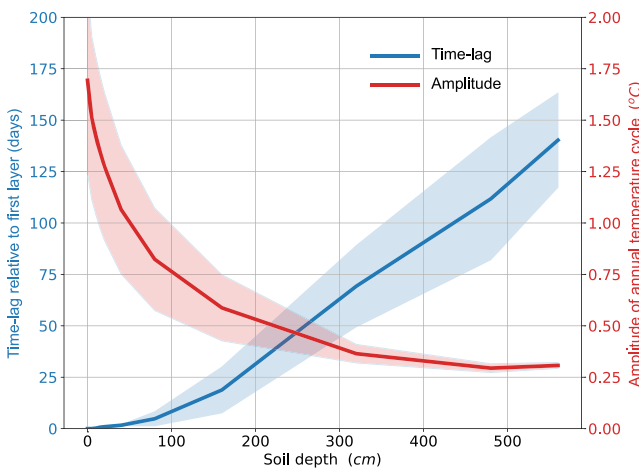


Figure 5. The difference between seasonal maximum and minimum soil temperature (red line and shade) and phase shift of annual cycle at different soil depths (blue line and shade), based on the daily soil temperature output in the Exp-1 simulation. Solid lines indicate the average across the TP, and the shades indicate the range of one standard deviation.

thermal inertia are. Moreover, 1-month lagged autocorrelation increases with soil column depth, indicating that anomalies in middle and deeper soil layers have higher month-to-month persistence in comparison to the upper soil layer.

Surface albedo affects LST by changing the surface-absorbed solar radiation. The anomalous LST and albedo in the current month are significantly correlated (Figure 4a). The sustained snow in the cold seasons leads to the long persistence of surface albedo, indicated by its high autocorrelation (Figure 4b). The 1-month lagged autocorrelation of surface albedo is 0.8 ($p < 0.01$), suggesting a high month-to-month persistence. As a result, LST anomaly is significantly correlated with surface albedo anomaly at 1-month lead, only slightly smaller than at 0-month lead (Figure 4a).

Since the observation only provided monthly mean data, and the station observations mostly located in the east TP, SSIb3-FSM outputs are used to provide the analyses for the entire TP at daily and monthly scales. The following discussion is based on Exp-1 products. Figure 5 shows the phase lag of the annual cycle at each soil layer relative to the surface layer, which is the time lag corresponding to the maximal cross correlation between the anomalies at the respective layers. It is an indicator of the days that the signal propagates from the surface to the respective layers. The simulated phase lag of the upper layers is less than 10 days. Therefore, anomaly in the upper layer is synchronous to the surface on the monthly scale, leading to a high correlation between them. It requires about 10–30 days for surface anomaly to propagate to the middle soil layers and more than 1–2 months into the deeper layers. Therefore, the lagged cross correlation between LST and SUBT at 0-month lead decreases with soil column depth. Meanwhile, the amplitude of the annual cycle, defined as the difference between the SUBT maximum and minimum (Amenu et al., 2005), decreases with soil column depth (Figure 5). The amplitude in the middle soil layer SUBT remains about half of that of the surface and damps to about 15% in the deep soil. In summary, the anomalous heat is stored in the middle soil layers with an adequate intensity and is interactive with LST in the current month.

Combined with the month-to-month persistence, SUBT anomaly in the middle soil layer can be preserved for months and has considerable impact on the LST in the current month. This inherent characteristic, therefore, results in high cross correlation between LST and middle-layer SUBT in leading months.

Over the entire TP, the SSIb3-FSM simulation (Exp-1) shows that the anomalies in the middle-layer SUBT and surface albedo at 1-month lead are significantly correlated to the LST anomaly (Figure 6). However, SW_{in} and LW_{in} at 1-month lead only show nonsignificant correlations to LST. The correlation between LST and LW_{in} at 1-month lead is less than 0.3 with discontinuities in nonsignificant areas.

The S2S predictability of middle-layer SUBT and surface albedo originates from the persistence in their autocorrelations. Based on the Exp-1 simulated time series averaged over the TP, the anomalies of SW_{in} and LW_{in} have memory of less than 10 days (Figure S3). Albedo anomaly persists 2–4 months in winter and spring. In particular, the anomalous surface albedo occurring in February and March has the longest memory, which persists for more than 3 months, highlighting its S2S predictability in late

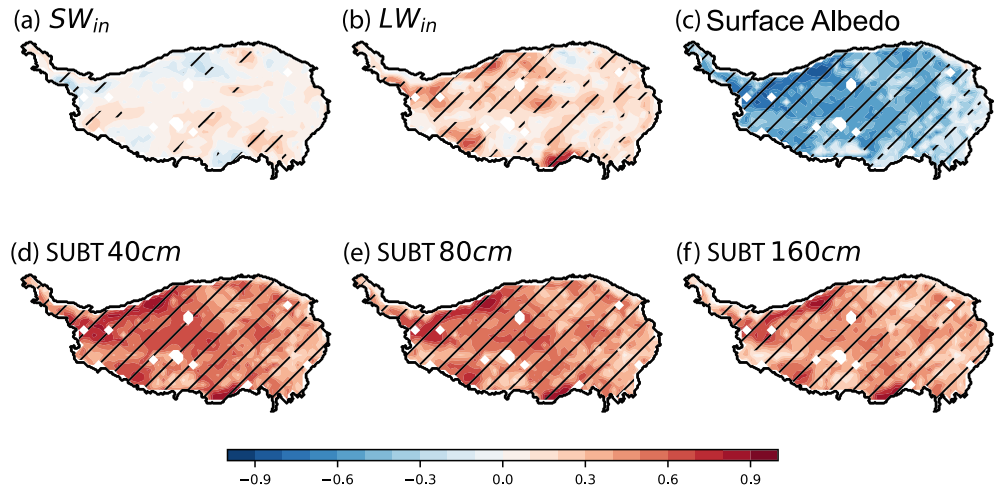


Figure 6. Cross correlation of LST to (a) SW_{in} , (b) LW_{in} , (c) surface albedo, and (d–f) middle-layer SUBT at 1-month lead based on the SSiB3-FSM forcing data and simulation (Exp-1). The hatches indicate the areas with significance level of 0.01.

spring and early summer. The memory of SUBT increases with soil column depth (Figure S3). At 20 cm, SUBT memory is about 10 days from January to October and about 20–30 days in November and December. SUBT at 40 to 80 cm has a memory of 1–2 months, with longer memory in cold seasons (up to 3 months). Anomalies at 160- to 320-cm SUBT persist longer than 3 months. Memory in SUBT and surface albedo are seasonally dependent. Anomalies in SUBT and surface albedo are monthly predictable in all calendar months and have S2S predictability in late spring and early summer. Considering the high simultaneous correlation of LST to SUBT and surface albedo, the predictability of LST anomaly is also implied.

3.3. Estimation of Monthly LST Anomaly Using Variables in the Previous Month

In this section, a LRM is employed to predict LST anomaly with input variables from the preceding month from the SSiB3-FSM meteorological forcing and Exp-1 simulation as predictors. LST is determined by the surface energy budget (Xue et al., 1996). With anomalies in primary surface energy-related variables in the preceding month as predictors, including SW_{in} , LW_{in} , surface albedo, LW_{out} , H_s , λE , and middle-layer SUBT at 40, 80, and 160 cm, hereafter referenced as All-Variables, the averaged R_{adj}^2 over TP is 0.46, based on the data from all calendar months (Figure 7a and Table 2). In some areas in the northwest, R_{adj}^2 is up to 0.80. The encouraging results indicate that LST is highly predictable at monthly scale with surface energy-related variables. The remaining variance can be explained by simultaneous interaction with predictors and other processes such as cloud, aerosols, SM, and vegetation phenology. With SUBT of the previous month as a predictor, the average R_{adj}^2 is 0.44 and shows a similar pattern as compared to All-Variables (Figure 7b). It is interesting to note that although with surface albedo alone, the LRM generates R_{adj}^2 of 0.34 (Table 2), and with both SUBT and surface albedo as predictors, R_{adj}^2 increases only slightly to 0.45. This finding supports the conjecture proposed by Xue et al. (2018) that a temporally filtered response to snow and surface albedo anomalies may be preserved in the SUBT. Furthermore, with LW_{in} alone as a predictor, R_{adj}^2 is 0.13, but no additional predictability increased when we used SUBT, surface albedo, and LW_{in} as predictors (Figure 7d and $R_{adj}^2 = 0.45$ in Table 2).

The effect of SM on land/atmosphere interaction has been widely investigated (Koster et al., 2004, 2006). In this study, we also assess the contribution of SM to the land memory. With SM of the previous month as a predictor, the average R_{adj}^2 is 0.19. When SM, SUBT, and surface albedo are combined for 1 month lead, explained variance only improves slightly (Table 2); however, for 2 months lead, R_{adj}^2 increases about 0.10 for most months (Table 2), suggesting that if we consider 2 months prediction, SM could enhance the soil memory by 0.1.

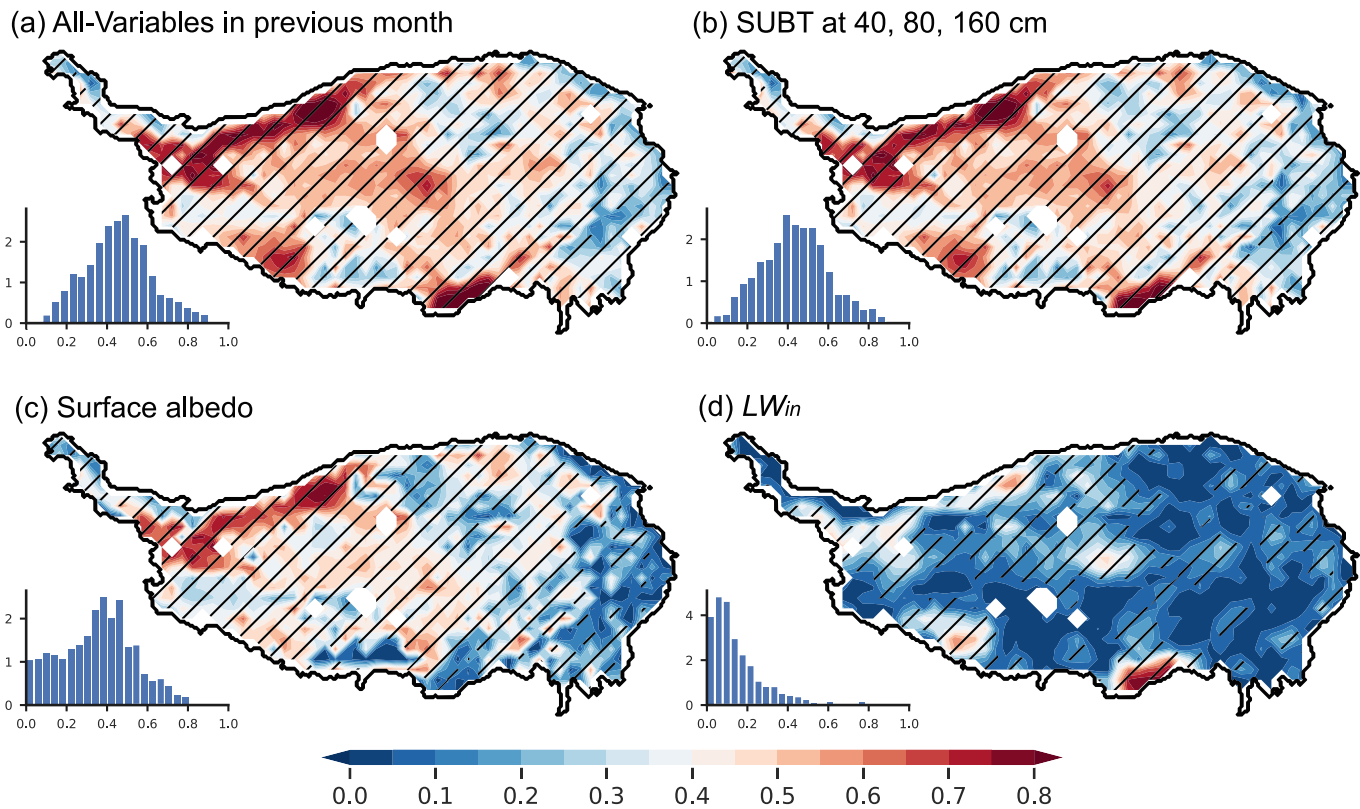


Figure 7. R^2_{adj} of linear regression model with input previous month variables of (a) All-Variables, (b) SUBT at 40, 80, and 160 cm, (c) surface albedo, and (d) LW_{in} . The histogram shows the probability density of spatial distribution in each prediction. The hatches denote the areas with $p < 0.01$.

Surface albedo and SUBT anomalies occurring in spring persist longer than in other seasons (Figure S3). Hence, the LRM shows better performance in predicting LST anomaly in spring. For instance, with All-Variables in April as predictors to predict LST in May, the average R^2_{adj} is 0.43 (Table 2). It also shows higher predictability over the central and western TP (Figure 8a). In the eastern TP, vegetation growth starting in May (Yu et al., 2010) largely changes surface energy budget and water balance (Liu et al., 2016), which involves a new factor affecting May LST anomaly. Meanwhile, cloud activity, especially convective cloud occurrence in the eastern TP in May (Li et al., 2019), alters downward solar radiation and affects LST. In contrast, because of the high month-to-month persistence of surface albedo and SUBT and less influence of vegetation and cloud activities, LST is more predictable in the central and western TP. With middle-layer

Table 2

R^2_{adj} for LST Prediction in All Months, March, April, and May With Predictors 1 and 2 Months Ahead

	All months		March		April		May	
	1 month	2 months	1 month	2 months	1 month	2 months	1 month	2 months
All-Variables	0.46	0.29	0.57	0.50	0.58	0.45	0.43	0.42
SUBT (40, 80, 160 cm)	0.44	0.26	0.48	0.43	0.51	0.37	0.36	0.34
Surface albedo	0.34	0.18	0.37	0.28	0.34	0.24	0.28	0.23
LW_{in}	0.13	0.10	0.19	0.18	0.29	0.18	0.17	0.16
Soil moisture (SM)	0.19	0.19	0.29	0.29	0.27	0.27	0.22	0.22
SUBT and albedo	0.45	0.27	0.52	0.46	0.53	0.40	0.39	0.37
SUBT, albedo, and LW_{in}	0.45	0.28	0.52	0.47	0.55	0.41	0.41	0.39
SUBT, albedo, and SM	0.48	0.37	0.59	0.56	0.58	0.50	0.44	0.43
All-Variables and SM	0.49	0.38	0.63	0.58	0.63	0.53	0.47	0.47

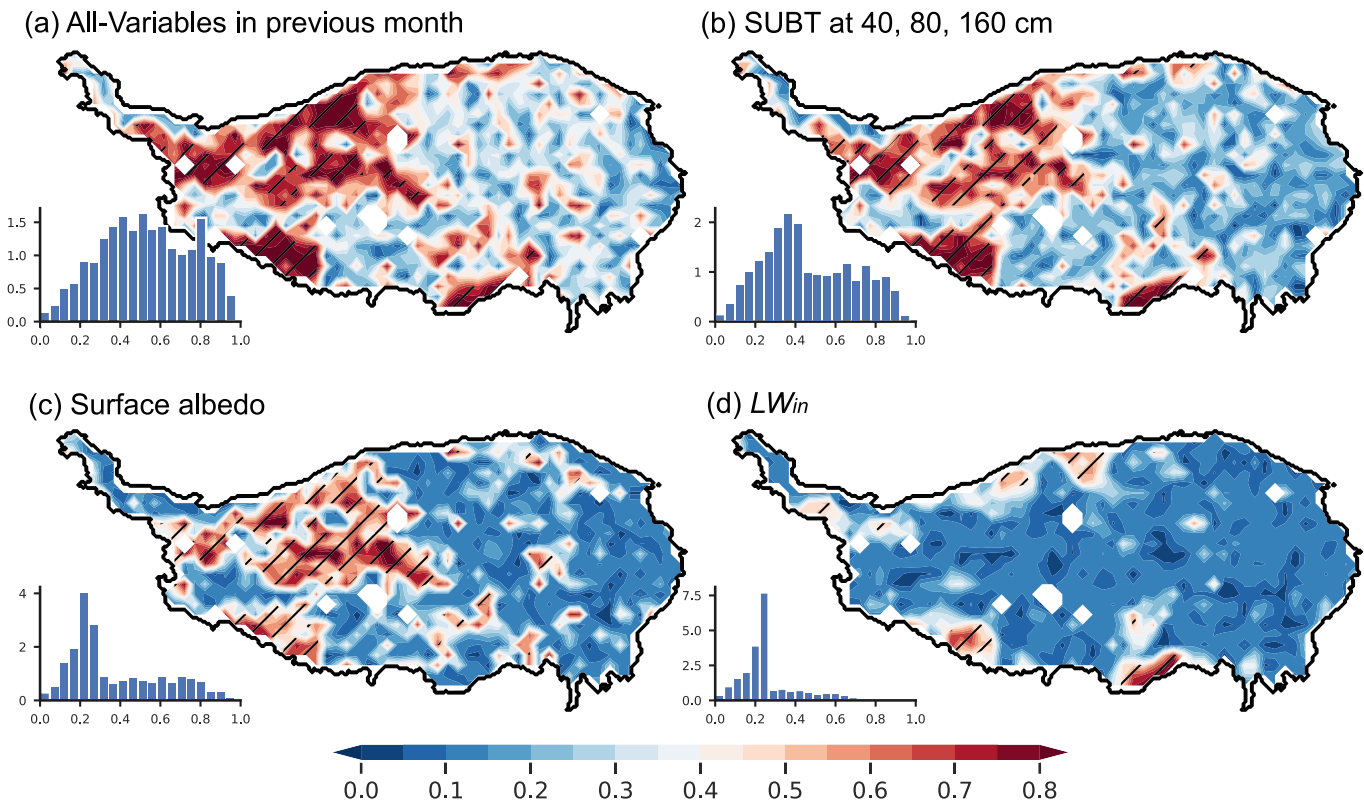


Figure 8. The same as Figure 7, except for May LST anomaly, and the LRM is fed by variables in April.

SUBT as a predictor, the average R_{adj}^2 is 0.36 (Table 2). R_{adj}^2 is slightly improved when surface albedo anomaly is included. For the LST anomaly in March and April, the results show a similar pattern and slightly higher R_{adj}^2 as compared to May (Table 2).

With All-Variables 2 months ahead, the average R_{adj}^2 reduces to 0.29 for all month LST prediction (Table 2). R_{adj}^2 of 2-month prediction with SUBT as a predictor is 0.26, based on the data from all calendar months. However, for March, April, and May, the explained variances are only slightly reduced compared to 1-month prediction with All-Variables, suggesting the great potential of SUBT as a predictor for S2S prediction.

The average MAE and RMSE over the TP are listed in supporting information Tables S1 and S2, respectively. The average MAE over the TP ranges in 1.42–1.83°C, and the average RMSE varies in 1.87–2.42°C, based on data from all calendar month for both 1- and 2-month prediction. The average MAE and RMSE ranges 1.47–2.32°C and 1.76–2.71°C for prediction in March, April, and May, respectively (Table S1 and S2). One predictor prediction generally produces larger MAE and RMSE, and the largest values are found when LW_{in} is used as only predictor (Table S2 and Figure S4).

3.4. Mechanisms of Snow and Surface Albedo Effect on LST

We have shown the capability of albedo and middle-layer SUBT to predict LST anomaly at the monthly and seasonal scale. In this and the following section, we explore the possible mechanisms.

During the cold season, TP snow anomalies have high month-to-month persistence (Figure 2). Strong snow anomaly can be formed in antecedent November and then persist through early summer (Wang et al., 2019). Because of snow albedo effect, surface albedo is significantly correlated to SWE in the current and preceding months. However, according to SSiB3-FSM simulation, the anomalous SWE changes (i.e., snowfall accumulation and snowmelt, referenced as SWEC) in November, December, February, and May have a larger impact on surface albedo anomaly than other months in the cold seasons (Figure 9). For instance, April surface albedo anomaly corresponds to the SWEC in December, February, and March, while there is no

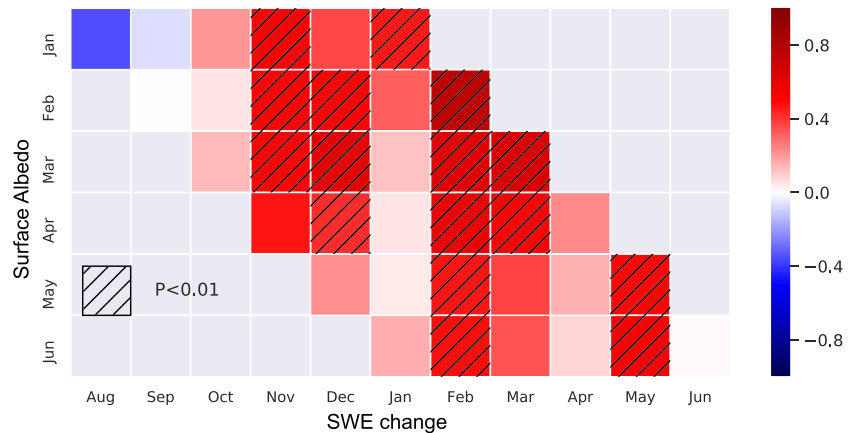


Figure 9. Lagged cross correlation between anomalous surface albedo and SWE change, based on Exp-1 output averaged across the TP. Hatches indicate the correlation with significance level at $p < 0.01$.

significant connection to January SWEC. Anomalous albedo in May and June are only significantly correlated to anomalous SWEC in February and May, which suggests the anomalous snowfall in February and snowmelt in May predominate surface albedo anomaly in late spring and early summer.

In order to quantify the effects of snow and surface albedo anomalies on LST anomaly, we also conducted paired experiments in which SWE was replaced by the average of extreme warm years (referenced as SWE-warm) and the average of extreme cold years (referenced as SWE-cold) in preceding months. The extreme years are selected based on LST anomaly of the target month, that is, May, as discussed in section 3.1. We conduct the Exp-2 simulation as introduced in section 2.3 for the sensitivity experiments using SSIb3-FSM and climatological forcing. The initial condition from this study is derived from a 60-year spin-up run similar to that discussed in Liu et al. (2019). The SSIb3-FSM is integrated from December to May. The simulation is repeated six times for the warm/cold years, with the simulated SWE being replaced by SWE-warm/SWE-cold 1 month per run. The difference between snow-warm and snow-cold runs is calculated to assess the effects of SWE in the respective preceding month on May LST. The effect of SWE change can be derived by comparing simulations with SWE imposed in two consecutive months. For convenience, we use Δ to represent the difference of snow-warm minus snow-cold.

The results show that less snow in December and January causes about 0.2°C more warmth in May (Figure 10). With Δ SWE imposed in December and driven by climatological forcing, simulated Δ SWE in January is close to the difference between extreme warm and cold years (Figures 11a–11c). The anomalous less snowfall in February additionally causes less SWE in February as compared to simulations with Δ SWE imposed in January (Figures 11d–11f), resulting in 0.3°C additional warmth in May. No distinct Δ SWEC

occurs in February to April. Therefore, Δ SWE in these months has similar contributions to May LST (about 0.5°C). The anomalous snowmelt in May induces about 1.0°C additional warmth compared to the SWE anomaly imposed in February to April (Figure 11g–11i), which results in 1.48°C warming in May. The simulated surface albedo shows persistent negative difference between snow-warm and snow-cold simulations. Δ Albedo in May induced by Δ SWE in preceding months coincides with Δ LST. The sensitivity experiments confirm the above statistical relationship, suggesting Δ SWEC in February and May predominate LST anomaly through the alteration of surface albedo.

Analogously, we conducted similar sensitivity experiments for the LST anomaly in April. SWE imposed in February, March, and April cause greater than 0.8°C Δ LST in April. Δ SWEC from March to April only contributes 0.05°C warming, while Δ SWEC in December, February, and

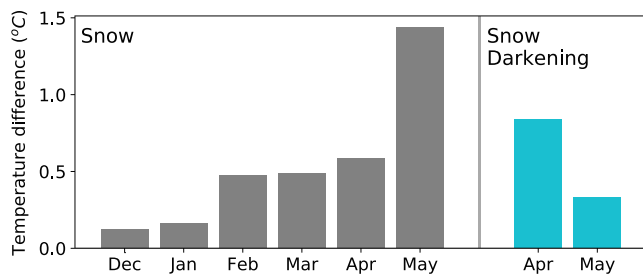


Figure 10. LST difference between snow-warm and snow-cold experiment. Gray bars indicate LST difference in May caused by SWE difference induced in preceding months. The blue bars denote the LST difference in May caused by snow darkening.

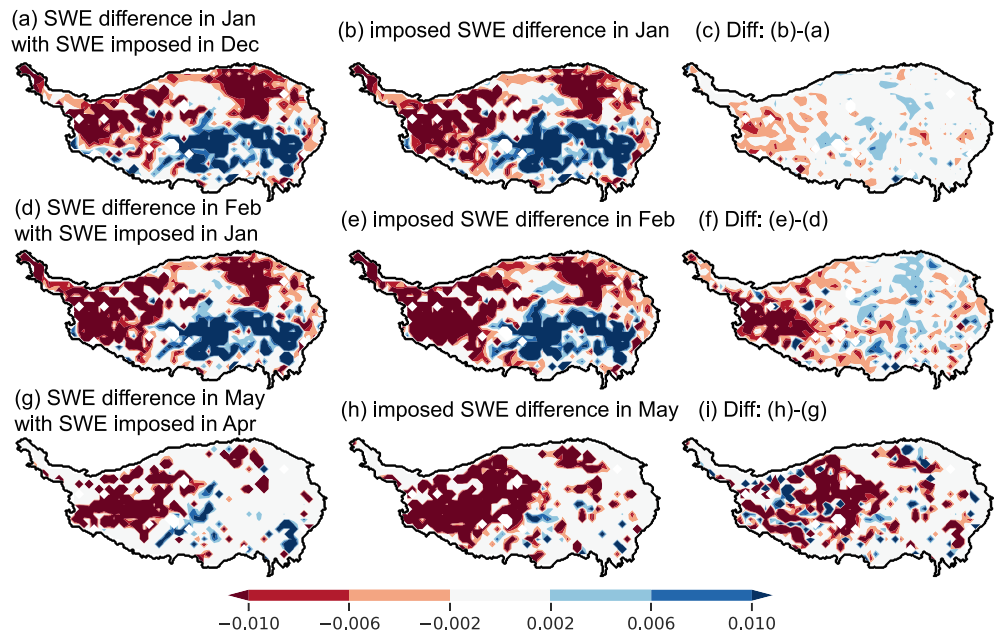


Figure 11. SWE difference between warm and cold years in (a) January generated by simulation with SWE imposed in December, (b) January, and (c) difference between (b) and (a) indicating the anomalous SWE changes occurring in January. (d–f) the same as (a)–(c) but for February and (g–i) for May.

March causes greater than 0.3°C warming in April, respectively. It also turns out that the snow effect is realized through the albedo effect and is consistent with the statistical relationship.

In addition, snow-darkening effect induced by aerosols in snow remarkably reduces the surface albedo during the snow melting period (Lau & Kim, 2018; Oaida et al., 2015), which increases surface absorbed solar radiation, leading to increase in surface temperature and enhanced snowmelt. To test the snow-darkening effect (snow-darkening run), we reduce surface albedo, when snow depth > 5 cm, in April and May by 0.2 based on Lau and Kim's (2018) snow-aerosol study. The difference from the simulation without such modification reveals the snow-darkening effect. The result shows that the snow-darkening effect leads to 0.8°C and 0.3°C warming in April and May, respectively.

3.5. Mechanisms of SUBT Effect on LST

SUBT has shown the ability to preserve LST anomaly and can be used as a predictor for monthly and seasonal predictions. In this section, we select June for discussion since it is a month of focus in current LST/SUBT studies (Xue et al., 2012, 2016, 2018). As discussed in section 3.2, the warm/cold years are selected based on LST anomaly in each month. Then we calculate the differences in ground heat flux, LST, and SUBT in 0-month lag (June, referenced as L_0), -5 to -1 -month lag (from January through May, referenced as L_{-5} to L_{-1}), and 1- to 5-month lag (from July through November, referenced as L_1 to L_5). Since the differences for any pair of warm and cold years show similar patterns, Figure 12 only shows their average. Before the LST anomaly reaching its maximum in L_0 , that is, June, the warmed surface keeps heating the soil, indicated by the positive ground heat flux in current (L_0) and preceding months (L_{-5} to L_{-1}). Anomalous energy propagates to middle to deeper soil. Because of the soil thermal persistence, anomalous warming is preserved in the soil layers. After the LST anomaly reaches its maximum, it decreases due to the interaction with the atmosphere, while SUBT anomaly is preserved due to soil thermal inertia. Hence, subsurface soil becomes warmer than the surface. As a result, the soil gradually releases the anomalous energy and continually heats the surface, indicated by the negative ground heat flux.

Furthermore, we investigated the sensitivity of SUBT persistence to soil thermal diffusivity ($D = \lambda/c$) and upper and lower boundary conditions. Soil heat transport is governed by the heat transfer equation:

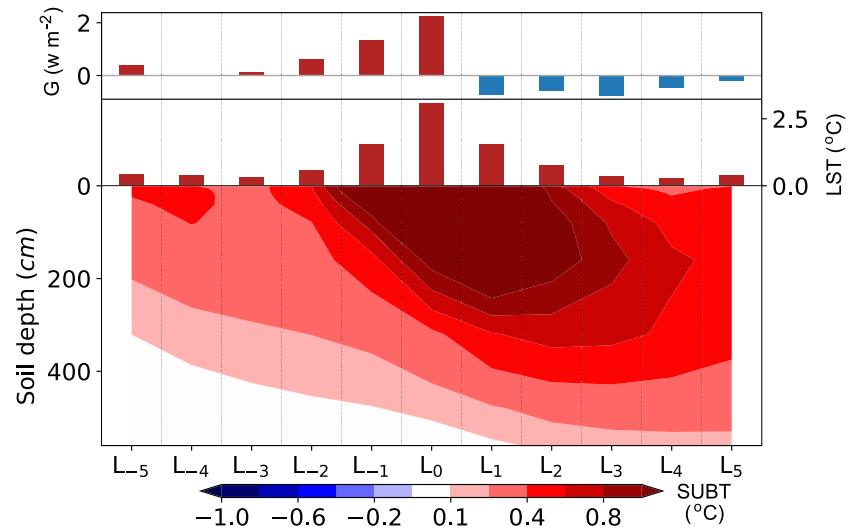


Figure 12. Difference in G, LST, and SUBT between the years with warm and cold months, based on Exp-1 products.

$$\rho \frac{\partial T_{z,t}}{\partial t} = \frac{\lambda}{c} \frac{\partial^2 T_{z,t}}{\partial z^2}, \quad (3)$$

where, $T_{z,t}$ is soil temperature over the vertical coordinate z and time t , λ is the soil thermal conductivity, and c is the volumetric heat capacity. $T_{z,t}$ can be determined when boundary and initial conditions and D are given. Given an initial soil temperature profile, the persistence of soil temperature is determined by upper and lower boundary conditions and the soil property.

To simplify simulation with a particular focus on thermal transport, we use SSiB3-Dry, in which all hydrologic processes are eliminated. We conduct four sets of experiments, which are similar to Exp. 2, but using SSiB3-Dry with climatological forcing. In the control run, SSiB3-Dry is integrated for 1 year without any modification. In the first sensitivity run (Exp-3.1), a vertical homogenous 5°C anomaly is imposed at the first time step and then integrated for 1 year. The difference shows the evolution of the imposed anomaly. In another three sensitivity experiments, all with imposed homogeneous 5°C initially, the soil thermal diffusivity is set to half of the control simulation to test the effect of soil property (Exp-3.2); a constant 2-m snow cover is imposed to test the effect of upper boundary conditions (Exp-3.3); and the total soil column depth is set to 3 m instead of 6 m from the control simulation to test the effect of lower boundary conditions (Exp-3.4).

The results show that, in Exp. 3.1, SUBT anomaly in the middle layers (for instance, 1 m) reduces rapidly in the first 20 to 40 days, then lasts for several months with lower amplitude (Figure 13a). The soil thermal persistence increases with decreased soil diffusivity, while the anomalous amplitude increases by about 30% in the first 40 days compared to the control simulation (Exp-3.2). The reduced thermal diffusivity implies an increase in soil heat capacity and/or a decrease in soil thermal conductivity. The former indicates a larger total thermal energy stored in soil layers, while the latter indicates lower thermal conduct efficiency, and both contribute to increasing the soil thermal persistence. With reduced total soil column depth (Exp-3.4), the anomalous amplitude decreases at a similar rate as the control in the first 20 days but reduces much faster thereafter. It confirms that the long memory in deeper soil helps to preserve SUBT anomaly in shallower layers. For the upper boundary condition sensitivity experiment (Exp. 3.3), the effect of snow insulation slightly increases soil thermal persistence by weakening the atmospheric forcing. Note that snow albedo feedback and its associating persistence are not inferred in this test. Zhang et al. (2018) reported that the atmospheric forcing on soil temperature is weakened by increased snow depth.

Soil thermal diffusivity is affected by soil constituent and hydrologic conditions (Li et al., 2010). We further investigate the sensitivity of soil thermal diffusivity to soil sand-clay ratio, soil ice content, SM, and soil organic carbon (SOC). The result shows that sand-clay and soil ice content have less impact on the

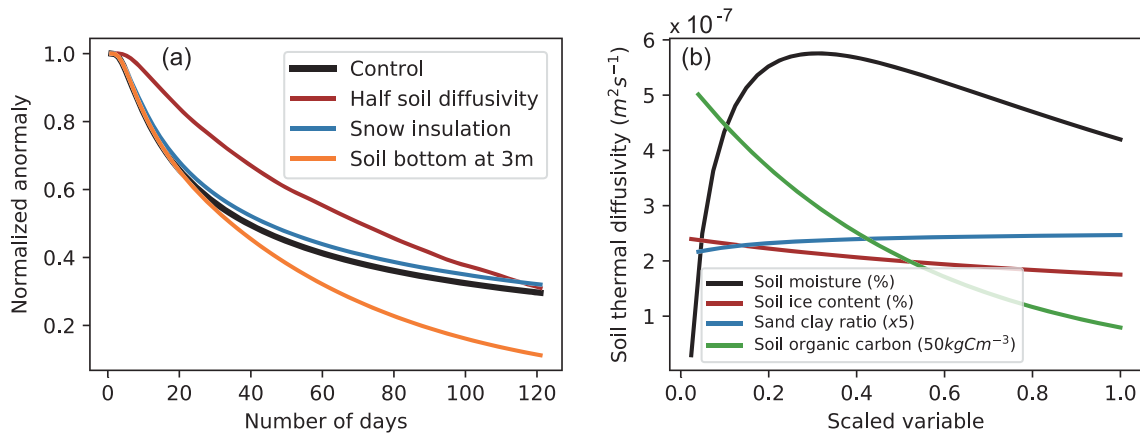


Figure 13. (a) Soil temperature anomaly at 1 m and (b) relationship between soil thermal diffusivity and soil moisture, soil ice content, sand-clay ratio, and soil organic carbon.

thermal diffusivity (Figure 13b). Soil thermal diffusivity increases rapidly with SM when SM is low. Soil thermal diffusivity reaches its maximum when SM is about 0.3. It then decreases with SM increase. When there is more SOC in soil, there is less soil thermal diffusivity.

4. Conclusion

In this study, we applied observed and simulated data over the Tibetan Plateau to investigate the characteristics of the LST anomaly and memory and their relationships to surface albedo, SUBT, and their associated snow and soil thermal processes. The anomalies in LST, snow and surface albedo, and SUBT over the TP exhibit long persistence. LST anomaly is highly correlated to anomalous snow, surface albedo, and SUBT in the current and preceding months. Meanwhile, anomalies in surface albedo and middle SUBT have a memory of 1–3 months based on data from all calendar months. The durations of the anomalies are significantly longer in winter and spring. Those relationships indicate surface albedo and SUBT are predictable at a monthly scale and show seasonal predictability especially when the anomalies occur in winter and spring. Moreover, our results suggest that surface albedo and middle-layer SUBT can be used to predict LST anomaly at the monthly and seasonal scales.

With surface albedo and middle-layer SUBT at 1-month lead as a predictor, the LRM explains almost the same variance of LST in the current month as compared to those with all primary surface energy relevant variables being included, with R_{adj}^2 of 0.44 based on data from all calendar months, and, in particular, with R_{adj}^2 of about 0.50 for spring prediction. R_{adj}^2 for predictors in 2-month lead is reduced by about 0.20 for all calendar month prediction, with significantly less reduction for spring prediction compared to the respective 1-month prediction. The encouraging performance of spring LST prediction with middle-layer SUBT and surface albedo as predictors also implies their important role as the initial condition for both weather and climate models (Diallo et al., 2019; Xia et al., 2013; Xue et al., 2016, 2018). The SM's contribution to extreme warm and cold years' soil memory has also been investigated. Their effect on the soil memory seems secondary in our cases, which is consistent with Robock et al.'s (2003) study. They found that although Asian snow albedo feedback is always operating, the anomalous snow cover impacts were not prolonged by SM feedbacks. More studies are needed to investigate for different climate conditions and different years.

In addition to the snow initial condition, our result also shows that snowfall in February and March and snowmelt in May have predominant effects on surface albedo and LST anomaly in May. Zhang et al. (2019) showed the statistical linkage between late-spring LST and February to April snow cover and their connection to the Arctic Oscillation. Aero in snow also contributes to increasing LST during the snowmelt period by up to 0.8°C. Lau and Kim (2018) reported that this snow-darkening effect induced TP warming in conjunction with the East Asian monsoon.

Changes in soil properties and upper and lower boundary conditions can largely alter soil memory. Our results confirm the important role of SUBT memory in reproducing SUBT anomaly decaying rate. Increased soil column depth contributes to increasing soil memory for all layers, which is consistent with Amenu et al. (2005), who show that the deeper soil records low-frequency (interannual and annual) signals and exerts an impact on the surface anomaly.

Thus far, a common shortcoming in the LS4P models has been their deficiency in holding the observed LST anomalies in terms of their persistence and intensity. This study intends to explore the possible causes of these weakness, in particular the causes of failing in preserving soil memory. This study reveals the important role of SUBT and snow anomalies in preserving the soil memory. Moreover, adequate soil thermal diffusivity and total soil column depth, which affects the soil heat capacity and the heat transport in the model, are two crucial parameters determining the SUBT anomaly persistence in simulation. Soil thermal diffusivity is highly sensitive to SM and SOC content, both of which, however, lack records over the TP and other mountain regions. More measurements are necessary.

This is an off-line study. Although the model in this study can properly reproduce surface and soil processes over the TP and is able to assess the key components that may affect the soil memory, the lack of atmospheric feedback should be noted. Further tests with fully coupled models are designed.

Conflict of Interest

The authors declare no competing interests.

Data Availability Statement

The output data from model integrations described here are available online (from <https://doi.org/10.17632/dvtmn59xft.1>). The station and gridded LST data were obtained online (from https://data.cma.cn/data/cdcdetail/dataCode/SURF_CLI_CHN_MUL_MON.html and http://data.cma.cn/data/cdcdetail/dataCode/SURF_CLI_CHN_TEM_MON_GRID_0.5.html), GLASS albedo product was obtained online (from <http://www.glass.umd.edu/Download.html>), and the meteorological forcing data were obtained online (from <https://data.tpdc.ac.cn/en/data/1980e33d-8615-448c-80e3-cfcb635fb110/?q=Yang%20Kun>).

Acknowledgments

This work was supported by NSF Grants AGS-1419526 and AGS-1849654. The authors acknowledge Cheyenne (doi:10.5065/D6RX99HX) provided by NCAR CISL, for providing HPC resources.

References

- Amenu, G. G., Kumar, P., & Liang, X. Z. (2005). Interannual variability of deep-layer hydrologic memory and mechanisms of its influence on surface energy fluxes. *Journal of Climate*, *18*(23), 5024–5045. <https://doi.org/10.1175/jcli3590.1>
- Bamzai, A. S., & Shukla, J. (1999). Relation between Eurasian snow cover, snow depth, and the Indian summer monsoon: An observational study. *Journal of Climate*, *12*(10), 3117–3132. [https://doi.org/10.1175/1520-0442\(1999\)012<3117:RBESCS>2.0.CO;2](https://doi.org/10.1175/1520-0442(1999)012<3117:RBESCS>2.0.CO;2)
- Dey, B., & Bhanu Kumar, O. S. R. U. (1983). Himalayan winter snow cover area and summer monsoon rainfall over India. *Journal of Geophysical Research*, *88*(C9), 5471–5474. <https://doi.org/10.1029/JC088iC09p05471>
- Diallo, I., Xue, Y., Li, Q., De Sales, F., & Li, W. (2019). Dynamical downscaling the impact of spring western US land surface temperature on the 2015 flood extremes at the Southern Great Plains: Effect of domain choice, dynamic cores and land surface parameterization. *Climate Dynamics*, *53*(1–2), 1039–1061. <https://doi.org/10.1007/s00382-019-04630-6>
- Dickinson, R. E. (1988). The force-restore model for surface temperatures and its generalizations. *Journal of Climate*, *1*(11), 1086–1097. [https://doi.org/10.1175/1520-0442\(1988\)001<1086:Tfmfst>2.0.CO;2](https://doi.org/10.1175/1520-0442(1988)001<1086:Tfmfst>2.0.CO;2)
- Dirmeyer, P. A., Schlosser, C. A., Brubaker, K. L., Dirmeyer, P. A., Schlosser, C. A., & Brubaker, K. L. (2009). Precipitation, recycling, and land memory: An integrated analysis. *Journal of Hydrometeorology*, *10*(1), 278–288. <https://doi.org/10.1175/2008JHM1016.1>
- Fasullo, J. (2004). A stratified diagnosis of the Indian monsoon-Eurasian snow cover relationship. *Journal of Climate*, *17*(5), 1110–1122. [https://doi.org/10.1175/1520-0442\(2004\)017<1110:ASDOTI>2.0.CO;2](https://doi.org/10.1175/1520-0442(2004)017<1110:ASDOTI>2.0.CO;2)
- Groisman, P. Y., Knight, R. W., Karl, T. R., Easterling, D. R., Sun, B., & Lawrimore, J. H. (2004). Contemporary changes of the hydrological cycle over the contiguous United States: Trends derived from in situ observations. *Journal of Hydrometeorology*, *5*(1), 64–85. [https://doi.org/10.1175/1525-7541\(2004\)005<0064:CCOTHC>2.0.CO;2](https://doi.org/10.1175/1525-7541(2004)005<0064:CCOTHC>2.0.CO;2)
- Hu, Q., & Feng, S. (2004a). Why has the land memory changed? *Journal of Climate*, *17*(16), 3236–3243. [https://doi.org/10.1175/1520-0442\(2004\)017<3236:whlmc>2.0.CO;2](https://doi.org/10.1175/1520-0442(2004)017<3236:whlmc>2.0.CO;2)
- Hu, Q., & Feng, S. (2004b). A role of the soil enthalpy in land memory*. *Journal of Climate*, *17*(18), 3633–3643. [https://doi.org/10.1175/1520-0442\(2004\)017<3633:AROTSE>2.0.CO;2](https://doi.org/10.1175/1520-0442(2004)017<3633:AROTSE>2.0.CO;2)
- Koster, R. D., Dirmeyer, P. A., Guo, Z. C., Bonan, G., Chan, E., Cox, P., et al. (2004). Regions of strong coupling between soil moisture and precipitation. *Science*, *305*(5687), 1138–1140. <https://doi.org/10.1126/science.1100217>
- Koster, R. D., Guo, Z., Dirmeyer, P. A., Bonan, G., Chan, E., Cox, P., et al. (2006). GLACE: The Global Land-Atmosphere Coupling Experiment. Part I: Overview. *Journal of Hydrometeorology*, *7*(4), 590–610. <https://doi.org/10.1175/JHM510.1>
- Kripalani, R. H., Kulkarni, A., & Sabade, S. S. (2003). Western Himalayan snow cover and Indian monsoon rainfall: A re-examination with INSAT and NCEP/NCAR data. *Theoretical and Applied Climatology*, *74*(1–2), 1–18. <https://doi.org/10.1007/s00704-002-0699-z>
- Kuang, X. X., & Jiao, J. J. (2016). Review on climate change on the Tibetan Plateau during the last half century. *Journal of Geophysical Research: Atmospheres*, *121*, 3979–4007. <https://doi.org/10.1002/2015JD024728>

- Lau, W. K. M., & Kim, K. M. (2018). Impact of snow darkening by deposition of light-absorbing aerosols on snow cover in the Himalayas-Tibetan Plateau and influence on the Asian summer monsoon: A possible mechanism for the Blanford hypothesis. *Atmosphere*, 9(11), 438. <https://doi.org/10.3390/atmos9110438>
- Li, B., Yang, L., & Tang, S. (2019). Intraseasonal variations of summer convection over the Tibetan Plateau revealed by Geostationary Satellite FY-2E in 2010–14. *Journal of Meteorological Research*, 33(3), 478–490. <https://doi.org/10.1007/s13351-019-8610-3>
- Li, Q., Sun, S. F., & Xue, Y. (2010). Analyses and development of a hierarchy of frozen soil models for cold region study. *Journal of Geophysical Research*, 115, D03107. <https://doi.org/10.1029/2009JD012530>
- Li, W., Guo, W., Qiu, B., Xue, Y., Hsu, P. C., & Wei, J. (2018). Influence of Tibetan Plateau snow cover on East Asian atmospheric circulation at medium-range time scales. *Nature Communications*, 9(1), 4243. <https://doi.org/10.1038/s41467-018-06762-5>
- Liu, Q., Wang, L., Qu, Y., Liu, N., Liu, S., Tang, H., & Liang, S. (2013). Preliminary evaluation of the long-term GLASS albedo product. *International Journal of Digital Earth*, 6(sup1), 69–95. <https://doi.org/10.1080/17538947.2013.804601>
- Liu, Y., Guo, W. D., & Song, Y. M. (2016). Estimation of key surface parameters in semi-arid region and their impacts on improvement of surface fluxes simulation. *Science China Earth Sciences*, 59(2), 307–319. <https://doi.org/10.1007/s11430-015-5140-4>
- Liu, Y., Xue, Y., MacDonald, G., Cox, P., & Zhang, Z. Q. (2019). Global vegetation variability and its response to elevated CO₂, global warming, and climate variability—A study using the offline SSIb4/TRIFFID model and satellite data. *Earth System Dynamics*, 10(1), 9–29. <https://doi.org/10.5194/esd-10-9-2019>
- Mahanama, S. P. P., Koster, R. D., Reichle, R. H., & Suarez, M. J. (2008). Impact of subsurface temperature variability on surface air temperature variability: An AGCM study. *Journal of Hydrometeorology*, 9(4), 804–815. <https://doi.org/10.1175/2008JHM949.1>
- Oaida, C. M., Xue, Y., Flanner, M. G., Skiles, S. M. K., De Sales, F., & Painter, T. H. (2015). Improving snow albedo processes in WRF/SSiB regional climate model to assess impact of dust and black carbon in snow on surface energy balance and hydrology over western U.S. *Journal of Geophysical Research: Atmospheres*, 120, 3228–3248. <https://doi.org/10.1002/2014JD022444>
- Park, H., Sherstiukov, A. B., Fedorov, A. N., Polyakov, I. V., & Walsh, J. E. (2014). An observation-based assessment of the influences of air temperature and snow depth on soil temperature in Russia. *Environmental Research Letters*, 9(6), 064026. <https://doi.org/10.1088/1748-9326/9/6/064026>
- Robock, A., Mu, M., Vinnikov, K., & Robinson, D. (2003). Land surface conditions over Eurasia and Indian summer monsoon rainfall. *Journal of Geophysical Research*, 108(D4), 4131. <https://doi.org/10.1029/2002JD002286>
- Vernekar, A. D., Zhou, J., & Shukla, J. (1995). The effect of Eurasian snow cover on the Indian monsoon. *Journal of Climate*, 8(2), 248–266. [https://doi.org/10.1175/1520-0442\(1995\)008<0248:TEOESC>2.0.CO;2](https://doi.org/10.1175/1520-0442(1995)008<0248:TEOESC>2.0.CO;2)
- Wang, B., Bao, Q., Hoskins, B., Wu, G., & Liu, Y. (2008). Tibetan Plateau warming and precipitation changes in East Asia. *Geophysical Research Letters*, 35, L14702. <https://doi.org/10.1029/2008GL034330>
- Wang, Z., Wu, R., Zhao, P., Yao, S., & Jia, X. (2019). Formation of snow cover anomalies over the Tibetan Plateau in cold seasons. *Journal of Geophysical Research: Atmospheres*, 124, 4873–4890. <https://doi.org/10.1029/2018JD029525>
- Wu, G. X., Zhuo, H. F., Wang, Z. Q., & Liu, Y. M. (2016). Two types of summertime heating over the Asian large-scale orography and excitation of potential-vorticity forcing I. Over Tibetan Plateau. *Science China Earth Sciences*, 59(10), 1996–2008. <https://doi.org/10.1007/s11430-016-5328-2>
- Wu, L., & Zhang, J. (2014). Strong subsurface soil temperature feedbacks on summer climate variability over the arid/semi-arid regions of East Asia. *Atmospheric Science Letters*. <https://doi.org/10.1002/asl2.504>
- Wu, R., & Kirtman, B. P. (2007). Observed relationship of spring and summer East Asian rainfall with winter and spring Eurasian snow. *Journal of Climate*, 20(7), 1285–1304. <https://doi.org/10.1175/JCLI4068.1>
- Wu, T. W., & Qian, Z. A. (2003). The relation between the Tibetan winter snow and the Asian summer monsoon and rainfall: An observational investigation. *Journal of Climate*, 16(12), 2038–2051. [https://doi.org/10.1175/1520-0442\(2003\)016<2038:TRBTW>2.0.CO;2](https://doi.org/10.1175/1520-0442(2003)016<2038:TRBTW>2.0.CO;2)
- Xia, Y., Ek, M., Sheffield, J., Livneh, B., Huang, M., Wei, H., et al. (2013). Validation of Noah-simulated soil temperature in the North American land data assimilation system Phase 2. *Journal of Applied Meteorology and Climatology*, 52(2), 455–471. <https://doi.org/10.1175/JAMC-D-12-033.1>
- Xiao, Z., & Duan, A. (2016). Impacts of Tibetan Plateau snow cover on the interannual variability of the East Asian summer monsoon. *Journal of Climate*, 29(23), 8495–8514. <https://doi.org/10.1175/JCLI-D-16-0029.1>
- Xue, Y., Boone, A., & Yao, T. D. (2019). Remote effects of high elevation land surface temperature on S2S precipitation prediction: First Workshop on LS4P and TPemIP. *GEWEX News* (Vol. 29, No. 1, pp. 14–16). Washington, DC: International GEWEX Project Office.
- Xue, Y., Lau, W. K. M., Yao, T., & Boone, A. (2019). Remote effects of Tibetan Plateau spring land surface temperature on global summer precipitation and its S2S prediction: Second Workshop on LS4P and TPemIP. *GEWEX News* (Vol. 29, pp. 8–10). Silver Spring, MD: International GEWEX Project Office.
- Xue, Y., Diallo, I., Li, W., David Neelin, J., Chu, P. C., Vasic, R., et al. (2018). Spring land surface and subsurface temperature anomalies and subsequent downstream late spring-summer droughts/floods in North America and East Asia. *Journal of Geophysical Research: Atmospheres*, 123, 5001–5019. <https://doi.org/10.1029/2017jd028246>
- Xue, Y., Ma, Y., & Li, Q. (2017). Land-climate interaction over the Tibetan Plateau. In *Oxford research encyclopedia of climate science* (pp. 1–31). NY, USA: Oxford University Press USA. <https://doi.org/10.1093/acrefore/9780190228620.013.592>
- Xue, Y., Oaida, C. M., Diallo, I., Neelin, J. D., Li, S., De Sales, F., et al. (2016). Spring land temperature anomalies in northwestern US and the summer drought over Southern Plains and adjacent areas. *Environmental Research Letters*, 11(4), 44,018. <https://doi.org/10.1088/1748-9326/11/4/044018>
- Xue, Y., Sellers, P. J., Kinter, J. L., & Shukla, J. (1991). A simplified biosphere model for global climate studies. *Journal of Climate*, 4(3), 345–364. [https://doi.org/10.1175/1520-0442\(1991\)004<0345:Asbmgf>2.0.Co;2](https://doi.org/10.1175/1520-0442(1991)004<0345:Asbmgf>2.0.Co;2)
- Xue, Y., Vasic, R., Janjic, Z., Liu, Y. M., & Chu, P. C. (2012). The impact of spring subsurface soil temperature anomaly in the western U.S. on North American summer precipitation: A case study using regional climate model downscaling. *Journal of Geophysical Research*, 117, D11103. <https://doi.org/10.1029/2012jd017692>
- Xue, Y., Zeng, F. J., & Schlosser, C. A. (1996). SSiB and its sensitivity to soil properties—A case study using HAPEX-Mobilhy data. *Global and Planetary Change*, 13(1–4), 183–194. [https://doi.org/10.1016/0921-8181\(95\)00045-3](https://doi.org/10.1016/0921-8181(95)00045-3)
- Yang, K., & Zhang, J. (2016). Spatiotemporal characteristics of soil temperature memory in China from observation. *Theoretical and Applied Climatology*, 126(3–4), 739–749. <https://doi.org/10.1007/s00704-015-1613-9>
- Yang, K., He, J., Tang, W., Qin, J., & Cheng, C. C. K. (2010). On downward shortwave and longwave radiations over high altitude regions: Observation and modeling in the Tibetan Plateau. *Agricultural and Forest Meteorology*, 150(1), 38–46. <https://doi.org/10.1016/j.agrformet.2009.08.004>

- Yao, T., Xue, Y., Chen, D., Chen, F., Thompson, L., Cui, P., et al. (2019). Recent Third Pole's rapid warming accompanies cryospheric melt and water cycle intensification and interactions between monsoon and environment: Multi-disciplinary approach with observation, modeling and analysis. *Bulletin of the American Meteorological Society*, *100*(3), 423–444. <https://doi.org/10.1175/BAMS-D-17-0057.1>
- Yu, H., Luedeling, E., & Xu, J. (2010). Winter and spring warming result in delayed spring phenology on the Tibetan Plateau. *Proceedings of the National Academy of Sciences of the United States of America*, *107*(51), 22151–22156. <https://doi.org/10.1073/pnas.1012490107>
- Zhang, T. (2005). Influence of the seasonal snow cover on the ground thermal regime: An overview. *Reviews of Geophysics*, *43*, RG4002. <https://doi.org/10.1029/2004RG000157>
- Zhang, X., Sun, S., & Xue, Y. (2007). Development of frozen soil model for climate study. *Journal of Hydrometeorology*, *8*(4), 690–701. <https://doi.org/10.1175/JHM605.1>
- Zhang, Y., Sherstiukov, A. B., Qian, B., Kokelj, S. V., & Lantz, T. C. (2018). Impacts of snow on soil temperature observed across the circumpolar north. *Environmental Research Letters*, *13*(4), 044012. <https://doi.org/10.1088/1748-9326/aab1e7>
- Zhang, Y., Zou, T., & Xue, Y. (2019). An Arctic-Tibetan connection on subseasonal to seasonal time scale. *Geophysical Research Letters*, *46*, 2790–2799. <https://doi.org/10.1029/2018GL081476>
- Zhao, P., Zhou, Z., & Liu, J. (2007). Variability of Tibetan spring snow and its associations with the hemispheric extratropical circulation and East Asian summer monsoon rainfall: An observational investigation. *Journal of Climate*, *20*(15), 3942–3955. <https://doi.org/10.1175/JCLI4205.1>